Environmental Science Nano

PAPER

Cite this: *Environ. Sci.: Nano*, 2019, **6**, 1207

Proteomics and antioxidant enzymes reveal different mechanisms of toxicity induced by ionic and nanoparticulate silver in bacteria†

Diana Barros, [ab] Arunava Pradhan, [ab] Vera M. Mendes, [c] Bruno Manadas,[c] Pedro M. Santos,[ab] Cláudia Pascoal[ab] and Fernanda Cássio *[ab]

Received 24th September 2018,
Accepted 24th February 2019

DOI: 10.1039/c8en01067f

rsc.li/es-nano

The increased use of silver nanoparticles (AgNPs) raises concerns about their impacts on aquatic ecosystems. The impacts of Ag^+ and AgNPs were assessed on proteomic and antioxidant enzymatic responses of *Pseudomonas* sp. M1. The effects of Ag^+ on bacterial growth were stronger than those of AgNPs (EC_{20} = 107.1 μg L^{-1} for Ag^+; EC_{20} = 307.2 μg L^{-1} for AgNPs), indicating the lower toxicity of the latter. At EC_{20}, the activities of antioxidant enzymes increased more under exposure to Ag^+ than to AgNPs, particularly for superoxide dismutase and glutathione peroxidase (stimulation of 667% and 433%, respectively). A total of 166 proteins were identified by SWATH-MS; among these, only 59 had their content significantly altered by one or both forms of silver. Exposure to AgNPs resulted in an increase of about 54% of these proteins, whereas 54% decreased under exposure to Ag^+. Gene Ontology enrichment analysis revealed that protein folding and transmembrane transport were the most relevant processes affected by Ag^+ exposure, whereas AgNPs mostly affected translation. Also, results suggest that each form of silver induced different adaptive responses. Furthermore, the low levels of Ag^+ released from AgNPs (<0.1%) support a minor role of dissolved silver in AgNP toxicity to *Pseudomonas* sp. M1.

Environmental significance

As the use of AgNPs increases, aquatic ecosystems can be a repository of this widely disseminated antimicrobial agent. Aquatic bacteria that play a crucial role in organic matter decomposition may come in contact with AgNPs through contaminated waters or contaminated organic matter. Moreover, it is still unclear whether the toxicity of AgNPs is related to their nanoparticulate form and/or mediated by Ag^+ released from AgNP dissolution. Based on proteomics, our study reveals that each form of Ag induced different adaptive responses in the metabolic, energetic and stress pathways. Of particular significance is the increased activity of superoxide dismutase and glutathione peroxidase, supporting the role of these enzymes in facing the oxidative stress induced by both forms of Ag.

Introduction

The developments in nanotechnology over the past decade increased concerns about the environmental impacts of engineered nanoparticles (ENPs). Silver nanoparticles (AgNPs) are among the most widely used ENPs.[1] Due to their broad-spectrum antimicrobial properties, AgNPs have been used extensively in textiles and therapeutics.[2,3] About 20–130 tons of ionic silver (Ag^+) were predicted to reach EU freshwaters per year, mainly due to ionic leaching of AgNPs from biocidal plastics and textiles.[4] The industrial production of AgNPs was predicted to become *ca.* 20 tons per year,[5] of which about 30% can be released to the aquatic environment.[6] The environmental concentrations of AgNPs in freshwaters are predicted to be lower than 1 μg L^{-1} but may increase up to 100 times in wastewater effluents.[7,8] Furthermore, the possibility of attaining higher AgNP concentrations due to accidental spills cannot be ignored. Hence, AgNPs have been considered emerging chemical contaminants in aquatic environments and recommended for environmental risk assessment.[9]

The prime challenge regarding the assessment of ENP toxicity in aquatic biota is still the establishment of standard nano-specific protocols,[10] including sample preparation and test conditions, to achieve reproducible results and to effectively link the toxicological information to the physicochemical properties of ENPs (but see test guidelines[11]).

[a] *Centre of Molecular and Environmental Biology (CBMA), Department of Biology, University of Minho, Campus of Gualtar, 4710-057 Braga, Portugal. E-mail: fcassio@bio.uminho.pt; Fax: +351253678980; Tel: +351253604045*
[b] *Institute of Science and Innovation for Bio-Sustainability (IB-S), University of Minho, Campus of Gualtar, 4710-057 Braga, Portugal*
[c] *CNC – Center for Neuroscience and Cell Biology, University of Coimbra, Portugal*
† Electronic supplementary information (ESI) available. See DOI: 10.1039/c8en01067f

Many studies have reported the toxic effects of AgNPs on freshwater organisms, including bacteria, algae, fungi, invertebrates and fish,[12–14] but little is known about the mechanisms underlying such effects. Some studies indicate that the bioavailable Ag^+ released from AgNPs contributes to toxicity.[15,16] Speciation of released Ag^+ in aquatic environments might be a key factor influencing toxicity and may occur *via* interactions with natural ligands, forming AgCl, Ag_2O, Ag_2S, and other silver(I) complexes.[17–20] Lubick[21] showed that some algal species are more sensitive to AgNPs than to free Ag^+, but when cysteine (a metal chelator) is added, the toxicity of both silver forms is reduced due to complexation of Ag^+. More recently, it was shown that actual Gibbs free energy can be used to accurately calculate the equilibrium concentrations of AgNPs and released Ag^+ and precisely determine the real transformation, fate, and ecotoxicity of AgNPs in aquatic environments.[19]

Heterotrophic bacteria play a crucial role in stream ecosystem processes, and they can be affected by acute and chronic exposure to AgNPs.[14,22] Very small particle size AgNPs can exhibit higher toxicity to prokaryotic cells than Ag^+ or other forms of Ag.[23,24] Chronic exposure to Ag^+ released from AgNPs at very low concentrations may also heighten the silver tolerance/resistance in bacteria.[25] Interactions with and adhesion of AgNPs to the bacterial surface can alter cell wall structure, and induce intracellular generation of reactive oxygen species (ROS), disruption of the plasma membrane, changes in protein interactions, and interference with DNA replication, and damage macromolecules (lipids, proteins, DNA and RNA).[18,19]

Environmental stress biomarkers and omics are among the most promising next-generation toxicity assessment tools, enhancing measurements of direct and highly sensitive responses to emerging environmental contaminants at the cellular and sub-cellular levels. Freshwater microbes and invertebrates are reported to trigger antioxidant defence mechanisms in response to exposure to metals or metal-based ENPs; these include changes in the activities of antioxidant enzymes such as catalase (CAT), superoxide dismutase (SOD), glutathione peroxidase (GPx), and glutathione-*S*-transferase (GST),[26–28] suggesting a role as oxidative stress biomarkers. These enzymes are closely associated with the ascorbate–glutathione cycle, in which the reduced form of glutathione (GSH) is converted to its oxidized form (GSSG), thus maintaining a high GSH : GSSG ratio. This is crucial for regulating the cellular redox state and preventing cellular damage by oxidative stress.[27,28] Proteomics can be used to unravel the dynamics of proteins in targeted organisms in response to environmental stressors, eventually revealing biomarkers of specific stressors.[29,30] Proteomics has been applied to environmentally relevant microbes, including aquatic bacteria, to reveal the mechanisms underlying the responses to anthropogenic stressors such as phenol, mancozeb and 2,4-dichlorophenoxyacetic acid,[31–33] making this approach valuable to determine the effects of emerging chemical contaminants. Adverse effects of AgNPs on *Pseudomonas* (*e.g. P. aeruginosa*, *P. putida*, and *P. chlororaphis*) have been reported,[34–37] but the mechanisms of toxicity have rarely been investigated.

The aim of this study was to investigate the impacts of AgNPs and their ionic precursor (Ag^+) on *Pseudomonas* sp. M1. This strain was chosen because of its heterotrophic nature and ability to biodegrade several environmental contaminants, including phenols, terpenes and other recalcitrant compounds.[32,38] To gain insights into the mechanisms underlying the impacts of Ag^+ and AgNPs on *Pseudomonas* sp. M1 and its ability to deal with these toxicants, we determined i) dose–response curves using bacterial growth as endpoint, ii) antioxidant enzymatic responses, and iii) proteomic responses. We hypothesized that i) *Pseudomonas* sp. M1 would exhibit more tolerance to AgNPs than to Ag^+, ii) the response profiles of antioxidant enzymes would potentially indicate the oxidative stress induced by the two silver forms, and iii) proteomic profiles would portray the key signature proteins in response to Ag^+ and AgNPs. Moreover, we aim to elucidate the role of dissolved ionic silver released from AgNPs in the overall toxicity effects as well as their underlying mechanisms.

Materials and methods

Bacterial exposure to Ag^+ and AgNPs

Pseudomonas sp. M1 is an oxidase-positive strain isolated from sediments of the Rhine River (Wageningen, Netherlands)[39] and phylogenetically close to the environmental strain *P. citronellolis*.[40] *Pseudomonas* sp. M1 cells were cultivated at 30 °C and maintained in *Pseudomonas* isolation agar (PIA) plates. For the exposure experiments, liquid cultures were prepared in sterile 250 mL Erlenmeyer flasks (presilanized to avoid adherence of metals/ENPs to the surface) with 50 mL of mineral medium (MM) as described by Hartmans *et al.*[41] and supplemented with 0.4% lactate as sole carbon source under orbital shaking (200 rpm; Certomat BS 3, B. Braun Biotech International) at 30 °C. The inoculum consisted of bacterial cells grown to an optical density (OD_{600}) of between 0.6 and 0.8 to reach the exponential growth phase and diluted in fresh MM containing lactate to obtain an initial OD_{600} of 0.15.

An aqueous suspension of citrate-coated AgNPs (1 g L^{-1}) was purchased from NanoSys GmbH (Wolfhalden, Switzerland). $AgNO_3$ (>99%) and other chemicals were purchased from Sigma-Aldrich (St. Louis, MO, USA) unless specified. A stock suspension of AgNPs (100 mg L^{-1}) was prepared in filtered (0.2 μm pore-size membrane; Millipore, Billerica, MA) ultrapure water (Milli-Q, 18.2 MΩ cm) and stored in the dark. A stock solution of $AgNO_3$ was prepared by suspending the powder in autoclaved (120 °C, 20 min) ultrapure water.

The estimations of the effective concentrations (EC_{10} and EC_{20}), using growth as endpoint, were performed by exposing *Pseudomonas* sp. M1 cells to increasing concentrations of AgNPs (≤1000 μg L^{-1}) and to their ionic precursor (Ag^+ in $AgNO_3$; ≤300 μg L^{-1}) for 90 min (at 30 °C, 200 rpm). For enzymatic and proteomic assays, cells at mid-exponential

phase[32,38] were exposed to toxicants (under same conditions). For enzymatic assays, cells were incubated with or without i) Ag^+ at concentrations similar to EC_{10} and EC_{20} and ii) AgNPs at concentrations similar to EC_{10} and EC_{20} for AgNPs and the concentrations used for exposure to Ag^+. For proteomic analysis, the cells were incubated under similar conditions with or without Ag^+ or AgNPs at the concentrations of their respective EC_{20}.

A complementary test was carried out with cysteine (L-cysteine, ≥98%, Sigma-Aldrich), a strong Ag^+ chelating agent, to better understand the actual role of released Ag^+ in AgNP-induced toxicity. The effects of 500 μM cysteine[14] on the growth of *Pseudomonas* sp. M1 in mineral medium with 0.4% lactate (30 °C for 90 min) was assessed in the presence or absence of Ag^+ (at EC_{20}) or AgNPs (at EC_{20}).

Characterization of nanoparticles and quantification of dissolved silver

The stock suspension of AgNPs was characterized using a UV-vis spectrophotometer (UV-1700 PharmaSpec, Shimadzu, Kyoto, Japan). The hydrodynamic size distribution, dispersity and stability of nanoparticles in the aqueous stock suspension before the experiment and in the exposure medium at the beginning and end of the experiment were monitored by dynamic light scattering (DLS) and zeta potential using a Zetasizer (Malvern, Zetasizer Nano ZS, Malvern Instruments Limited, UK).

Total and dissolved Ag^+ derived from AgNPs in the growth medium containing AgNPs were quantified at the beginning and at the end of the experiment by inductively coupled plasma mass spectrometry (Thermo X7 Q-ICP-MS, Thermo Scientific) at the Scientific and Technological Research Assistance Centre (C.A.C.T.I., University of Vigo, Spain).

Bacterial cells were removed from the medium by centrifugation (5000*g*, 5 min). Total Ag concentration (isotope ^{109}Ag) in the medium was determined in cell-free supernatant diluted with HNO_3 (2%). The quantification of dissolved Ag^+ from AgNPs was performed in cell-free supernatant after ultrafiltration for 30 min (3220*g*, 3 times) using Amicon Ultra-15 centrifugal filter units (Merck Millipore, Germany; 3 kDa molecular weight cut-off corresponding to <2 nm of estimated pore size) followed by acidification with HNO_3 (1.68% final concentration).

Preparation of cell-free extracts and protein quantification

Cells of *Pseudomonas* sp. M1 were harvested by centrifugation (15 000*g* for 10 min at 4 °C). For the assessment of the activities of antioxidant enzymes, cells were washed twice with ice-cold washing buffer (10 mM Tris-HCl, pH 7.0, 0.25 M sucrose) and resuspended into the sonication buffer (10 mM Tris-HCl, pH 7.0). For the proteomic analysis, 10 mM Tris-HCl (pH 7.4) with 0.25 M sucrose was used as washing buffer, whereas sucrose was not present in the sonication buffer. Cells were disrupted by ultrasonication at 20 kHz (15 min, cycles of 3 s burst with a 9 s interval, in ice) using a 13 mm probe and an Ultrasonic Processor GEX 400 (Sonics and Materials Inc, CT, USA). Unbroken cells were removed by centrifugation (5000*g* for 15 min at 4 °C), and cell-free extracts were obtained by centrifugation at 16 000*g* for 30 min at 4 °C followed by filtration (0.2 μm; Millipore, Billerica, MA). The extract was stored at −80 °C until use.

Protein concentration in the cell-free extracts was determined by a modified Lowry method[42] using bovine serum albumin (BSA) as protein standard.

Antioxidant enzyme activities

Antioxidant enzyme activities from unexposed cells were compared with those from cells exposed to Ag^+ or AgNPs by spectrophotometry (SpectraMax Plus 384 Microplate Reader, Molecular Devices, CA, USA). The activity of SOD was assessed based on its ability to inhibit superoxide radical dependent reactions using the Ransod Kit (Randox Laboratories Limited, Crumlin, UK). Briefly, 10 μL of the cell-free extract was added to 165 μL of reaction mixture containing 0.05 mM xanthine, 0.025 mM 2-(4-iodophenyl)-3-(4-nitrophenol)-5-phenyltetrazolium chloride (INT) dissolved in 40 mM 3-(cyclohexylamino)-1-propanesulfonic acid (pH 10.2) and 0.94 mM ethylenediaminetetraacetic acid (EDTA). The formation of superoxide radicals from xanthine started after the addition of 25 μL of xanthine oxidase (80 U L^{-1}).

The activity of CAT was determined as described by Clairborne.[43] 25 μL cell-free extract was added to a 275 μL reaction mixture comprising 0.05 M potassium phosphate buffer (pH 7.0) and 30 mM H_2O_2. The decrease in absorbance due to dismutation of H_2O_2 was detected at 240 nm (ε = 0.04 mM^{-1} cm^{-1}). CAT activity was calculated from the slope of the H_2O_2 absorbance curve and normalized to the protein concentration.

The GPx activity was determined according to Flohé and Günzler[44] with slight modifications.[28] Cell-free extract (10 μL) was added to the reaction mixture (290 μL) containing 0.05 M potassium phosphate buffer (pH 7.0), 1 mM EDTA, 1 mM NaN_3, 1 mM GSH (reduced glutathione), 0.24 mM reduced form of nicotinamide adenine dinucleotide phosphate (NADPH), 0.25 mM H_2O_2 and 0.2 U glutathione reductase (GR, from yeast). H_2O_2 served as the substrate while NaN_3 blocked the activity of catalase. The oxidation of NADPH was detected at 340 nm (ε = 6.2 mM^{-1} cm^{-1}) when GR reduced GSSG (oxidized glutathione) to GSH. The activity of GPx was calculated from the slope of the NADPH absorbance curve and normalized to the protein concentration.

The activity of GST in *Pseudomonas* sp. M1 was determined according to Habig *et al.*[45] by measuring the formation of 1-glutathion-2,4-dinitrobenzene resulting from the conjugation of GSH with 1-chloro-2,4-dinitrobenzene (CDNB). The cell-free extract (50 μL) was added to 250 μL of reaction mixture containing 0.1 M potassium phosphate buffer (pH 6.5), 1.5 mM CDNB and 1.5 mM GSH. The activity of GST was calculated from the slope of the absorbance curve at 340 nm (ε = 9.6 mM^{-1} cm^{-1}) and normalized to the protein concentration.

Protein denaturation, SDS-PAGE and gel staining

Prior to protein identification, volumes equivalent to 200 μg of total protein from each sample were incubated for 60 min at room temperature with urea loading buffer containing 9 M urea, 50 mM Tris at pH 8.8, 10% (v/v) glycerol, 10% (w/v) SDS, 0.002% (w/v) bromophenol blue and 20 mM dithiothreitol (DTT). A second incubation was done for 60 min at room temperature with the same buffer containing 20 mM acrylamide. Then, samples were loaded on SDS-polyacrylamide gels and subjected to electrophoretic separation. Finally, gels were stained with Coomassie Brilliant Blue G-250 solution. Detected protein bands were excised, sliced into small pieces and used for protein identification.

SWATH-MS analysis

After denaturation, the proteins were alkylated with acrylamide and subjected to in-gel digestion with trypsin (0.01 mg mL^{-1}) by using the short GeLC approach.[46] The formed peptides were subjected to SPE using OMIX tips with a C18 stationary phase (Agilent Technologies) as recommended by the manufacturer and then resuspended in 30 μL of mobile phase containing iRT peptides (Biognosys AG) as internal standards. Five μL of each replicate sample was combined to obtain one pooled sample per experimental condition (in a total of four pools) to be used for protein identification and SWATH-MS (sequential windowed data independent acquisition of the total high-resolution mass spectra)-library generation.

Samples were analyzed on a Triple TOFTM 5600 System (ABSciex®) in two phases: information-dependent acquisition (IDA) of the pooled samples for protein identification, and SWATH acquisition of each individual sample for protein quantification (see details in the ESI†). A specific library of precursor masses and fragment ions was created by combining all files from the IDA experiments and used for subsequent SWATH processing. Libraries were obtained using Protein Pilot™ software (v5.1, ABSciex®) searching against a database composed of the genus *Pseudomonas* from the SwissProt database (released at June 2015).

SWATH data processing was performed using the SWATH™ processing plug-in for PeakView™ (v2.0.01, ABSciex®). Briefly, peptides were selected automatically from the library and up to 15 peptides with up to 5 fragment ions were chosen per protein. Quantitation was attempted for all proteins in the library file that were identified below 5% local false discovery rate (FDR) from ProteinPilot™ searches by extracting the peak areas of the target fragment ions of those peptides using an extracted-ion chromatogram (XIC) window of 5 minutes with 20 mDa XIC width.

Peptides that met 1% FDR threshold in at least three out of the four biological replicates were retained, and the levels of the proteins were estimated by summing all the respective transitions and peptides that met the criteria (adapted from ref. 47). For comparisons between experiments, protein levels were normalized to the total intensity. The detailed process and description can be found in the ESI.†

Statistical analyses

The effective concentrations of Ag^+ and AgNPs inducing 10% or 20% of decrease (EC_{10} and EC_{20} with the respective 95% C.l.) in bacterial growth were calculated using PriProbit 1.63.[48] Data in percentages were arcsine square root transformed to achieve normal distribution and homoscedasticity before analyses of variance.[49]

The effects of cysteine and the form of silver (Ag^+ or AgNPs) were tested by two-way analyses of variance (ANOVAs) followed by Dunnett's *post hoc* tests to identify treatments that differed significantly from the control. Two-way ANOVAs were also used to test for the effects of AgNPs or Ag^+ concentrations on antioxidant enzymes. One-way ANOVAs were used to test for the effects of each form of silver (Ag^+ or AgNPs) on the protein contents. Analyses were done using Prism 7.0 for Windows (GraphPad Software Inc., CA, USA).

Fold changes of statistically significant proteins (one-way ANOVA, $P < 0.05$) were determined by log2 transformation of the ratio of protein levels under exposure to Ag^+ or AgNPs *versus* control conditions.

Heatmap and clustering analyses of significantly altered proteins were performed using GProX (version 1.1.15).[50] The proteins displayed in the heatmap were clustered according to their behavioural profiles. Clustering was performed using the unsupervised clustering fuzzy *c*-means algorithm implemented in the Mfuzz package,[51] a soft clustering algorithm, noise-robust and well-fitted to the protein profile data. Gene Ontology (GO) enrichment analysis was performed and the most representative biological processes associated with each cluster were highlighted. GO annotations for the 59 statistically altered proteins were performed using Blast2GO (version 4.1.9) where protein sequences were loaded as a Sequences (FASTA) file. The BLAST was performed against the NCBI non-redundant (nr) protein database using the BLASTP method. GO annotations were exported for the Biological Process category and imported to the GProX software to perform the enrichment analysis. Each cluster was tested for overrepresented GO compared with cluster 3 (background) using the binomial statistical test with the Benjamini–Hochberg adjustment ($P < 0.05$). Significant effects were determined by PERMANOVA.

Principal component analysis (PCA) was applied to coordinate the alterations in the proteins and the activities of antioxidant enzymes (SOD, CAT, GST and GPx) according to the treatments (control, Ag^+ and AgNPs). The proteins related to the stress response used in PCA were catalase-peroxidase (KatG) and alkyl hydroperoxide reductase subunit C (AhpC). Significant effects were determined by PERMANOVA. PCA was performed in PAST 3.14 for Windows (copyright Hammer & Harper, Ohio, USA[52]).

Results

Characterization of AgNPs and quantification of dissolved Ag^+

The AgNPs in mineral medium showed a peak at 419 nm by UV-vis spectrophotometry. At the beginning of the experiment, AgNPs at the highest concentration showed two peaks

of hydrodynamic diameter (HDD) of smaller (average HDD <45 nm; area intensity of 8.3%) and larger size range (average HDD <310 nm; area intensity of 91.7%; Table 1). The peak with the larger hydrodynamic size range was probably the consequence of AgNP agglomeration due to interactions with the medium components. After 90 min of exposure to AgNPs, only one peak was observed and the size of the larger particles increased indicating increased NP agglomeration. The zeta potential of the AgNPs (−20.9 mV), the conductivity and the electrophoretic mobility did not change after 90 min of exposure (initial *vs.* final conductivity: 7.38 ± 0.09 *vs.* 7.41 ± 0.03 mS cm^{-1}; and mobility: −1.39 ± 0.05 *vs.* −1.39 ± 0.04 μm cm V s^{-1}).

Changes in total silver quantification by ICP-MS in mineral medium either at the initial time (T0) or at the end of the experiment (T1 = 90 min) were not apparent (18.90 ± 0.71 μg L^{-1} at T0 and 21.68 ± 3.03 μg L^{-1} at T1; Table 1). Dissolved Ag^+ quantification by ICP-MS revealed that, at the beginning of the exposure (T0), the concentration of Ag^+ originating from the dissolution of AgNPs to the mineral medium (300 μg L^{-1} in 50 mL) was 0.30 ± 0.07 μg L^{-1}; however, at the end of the experiment (T1), the concentration of dissolved Ag^+ was lower than that at T0 (<0.2 μg L^{-1}; the detection limit was 0.06 μg L^{-1}).

Effects of Ag^+ and AgNPs on the growth of *Pseudomonas* sp. M1

The specific growth rate of *Pseudomonas* sp. M1 was 0.80 h^{-1}; the growth was inhibited by the exposure to Ag^+ and AgNPs. The increase in the concentration of Ag^+ or AgNPs resulted in a dose-dependent reduction of the specific growth rate (Fig. 1). Inhibitory effects of Ag^+ on the bacterial growth were more pronounced than those of AgNPs because EC_{10} and EC_{20} of Ag^+ were ~4.4 and ~2.9 times lower than that of AgNPs, respectively (Table 2).

The role of Ag^+ in the AgNP toxicity was further analysed by testing the effects of both forms of silver in the presence of an Ag^+ ligand (cysteine). Exposure to cysteine alone did not affect the bacterial growth ($P > 0.05$; Fig. S1†). In the absence of cysteine, exposure to Ag^+ or AgNPs at EC_{20} significantly inhibited bacterial growth ($P < 0.005$; Fig. S1†). The presence of cysteine did not alter the effect of AgNPs on *Pseudomonas* sp. M1 ($P > 0.05$) but alleviated the negative effect of Ag^+, showing no difference in bacterial growth from control ($P > 0.05$; Fig. S1†).

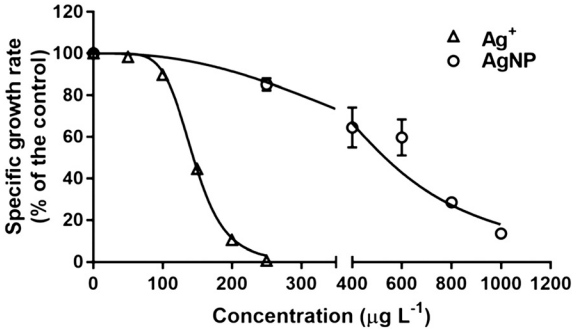

Fig. 1 Effects of AgNPs (circles) or Ag^+ (triangles) on the specific growth rate of *Pseudomonas* sp. M1. Data are percentages of the specific growth rate of the control culture in mineral medium with lactate at 30 °C. Mean ± SEM, $n = 3$.

Effects of Ag^+ and AgNPs on the activity of antioxidant enzymes

After 90 min of exposure of *Pseudomonas* sp. M1 to Ag^+ or AgNPs, the activities of all tested antioxidant enzymes, except for GST, increased significantly with concentration (two-way ANOVA, $P < 0.05$) of both silver forms (Fig. 2 and Table S1†). SOD and GPx activities increased significantly ($P < 0.05$) under Ag^+ or AgNPs exposure, particularly at the highest concentrations (Fig. 2A and B). GST activity did not differ significantly from control (Fig. 2A and B). At the same concentration (50 or 100 μg L^{-1}), stimulation of SOD and GPx activities by Ag^+ was stronger than by AgNPs (Fig. 2). When the enzyme activities were compared at the exposure concentrations closer to EC_{10} (50 μg L^{-1} for Ag^+; 200 μg L^{-1} for AgNPs), only SOD and GPx activities were significantly higher than in control upon exposure to Ag^+ (303.6% and 295.2%, respectively; Fig. 2A), whereas AgNPs strongly induced the activities of GPx (310.8%), SOD (283.2%) and CAT (268.7%) (Fig. 2B). When the cells were exposed to 100 μg L^{-1} Ag^+ (near EC_{20} of Ag^+: 107.1 μg L^{-1}), maximum activity was observed for SOD (667.1%) followed by GPx (418.3%) and CAT (274.3%) (Fig. 2A). At 300 μg L^{-1} AgNPs (EC_{20} of AgNPs: 307.2 μg L^{-1}), the activity of SOD was highest (583.4%) followed by that of GPx (433.8%), whereas CAT activity decreased (135.5%) to the control level (Fig. 2B).

Effects of Ag^+ and AgNPs on the proteome of *Pseudomonas* sp. M1

After 90 min of exposure of *Pseudomonas* sp. M1 to both forms of silver at concentrations (100 μg L^{-1} Ag^+ and 300 μg

Table 1 Zeta potential and hydrodynamic diameter (HDD) of AgNPs and total and dissolved Ag concentration in mineral medium with 0.4% lactate before (T0) and after 90 min (T1) of exposure to AgNPs at concentrations inhibiting 20% (EC_{20}) of the growth of *Pseudomonas* sp. M1. Mean ± SD, $n = 3$

Time	Zeta potential (mV)	PdI	Peak 1		Peak 2		Total Ag (μg L^{-1})	Dissolved Ag (μg L^{-1})
			HDD (nm)	Area intensity (%)	HDD (nm)	Area intensity (%)		
T0	−20.9 ± 0.7	0.56 ± 0.12	307.4 ± 36	91.7 ± 2	42.2 ± 27	8.3 ± 2	18.90 ± 0.71	0.30 ± 0.07
T1	−20.9 ± 0.6	0.50 ± 0.31	657.8 ± 33	100 ± 0	—	—	21.68 ± 3.03	<0.20 ± 0.00

PdI: polydispersity index.

Table 2 Concentrations of Ag^+ and AgNPs inhibiting 10% (EC_{10}) and 20% (EC_{20}) of the growth of *Pseudomonas* sp. M1 grown in mineral medium with 0.4% lactate at 30 °C for 90 min. (95% C.I. in parenthesis)

Stressor	EC_{10} (μg L^{-1})	EC_{20} (μg L^{-1})
Ag^+	51.2 (5.3–75.3)	107.1 (36.9–138.1)
AgNPs	225.7 (105.9–312.3)	307.2 (179.6–395.3)

L^{-1} AgNPs) similar to their respective EC_{20} on bacterial growth (EC_{20} = 107.1 μg L^{-1} for Ag^+ and EC_{20} = 307.2 μg L^{-1} for AgNPs), a total of 166 proteins were identified through SWATH-MS (Table S2†). Out of these, the contents of 59 proteins (35.5%) were significantly altered after exposure to Ag^+ or AgNPs (one-way ANOVA, $P < 0.05$; Table S2†). Among these 59 proteins, 27 increased and 32 decreased after exposure to Ag^+, whereas the opposite was found under AgNP exposure (*i.e.*, 27 decreased and 32 increased) (Fig. S2†). Moreover, the majority (74.6%) of the proteins whose contents were significantly altered showed a similar pattern (22 proteins increased; 22 proteins decreased) under exposure to both Ag forms. The average fold change of positively altered proteins was higher under exposure to Ag^+ (0.89-fold for Ag^+ *vs.* 0.58-fold for AgNPs), whereas the opposite was found for negatively altered proteins (−0.71-fold for Ag^+ *vs.* −1.87-fold for AgNPs).

A heatmap analysis shows the dynamic profiles of the proteins significantly altered (in the control and under exposure to Ag^+ and to AgNPs; Fig. 3A). Proteins were clustered according to their behavioural profiles and 4 clusters were generated (Fig. 3B).

Cluster 1 was represented by 13 proteins, which increased under exposure to AgNPs (average fold change: 0.61) and decreased under exposure to Ag^+ (average fold change: −0.29), except for 3 proteins (Table S2†). The contents of all proteins in cluster 2 (15 proteins) decreased under AgNP exposure (average: −1.44-fold), while under Ag^+ exposure, 5 proteins increased (average fold change: 0.38) and 10 proteins decreased (average: −0.27). All proteins in cluster 3 (12 proteins) decreased significantly under Ag exposure (average: −2.39-fold by AgNPs and −1.43-fold by Ag^+). Both silver forms stimulated (average: 0.56-fold by AgNPs and 1.05-fold by Ag^+) the proteins from cluster 4 (19 proteins).

Relationships between oxidative stress enzymes and related proteins

PCA of overall responses of antioxidant enzymes and proteins involved in antioxidant activities in *Pseudomonas* sp. M1 under exposure to EC_{20} of Ag^+ or AgNPs showed that PC1 and PC2 explained 70.8% and 19.6% of the total variance, respectively (Fig. 4). Exposure of the cells to Ag^+ and AgNPs led to significant effects on the activities of antioxidant enzymes and the contents of proteins with antioxidant activities (PERMANOVA, $P < 0.05$). PCA showed a clear discrimination between controls and treatments with Ag^+ or AgNPs along the PC1 based on the responses of oxidative stress biomarkers. PC2 segregated Ag^+ from AgNPs. With the exception of AhpC, all oxidative stress biomarkers were positively associated with Ag^+ or AgNPs. CAT and KatG were closely associated with each other and were positively correlated to Ag^+, whereas GPx, SOD and GST were associated with both treatments.

Discussion

Our study showed that short-term exposure to both Ag^+ and AgNPs had negative impacts on the growth of *Pseudomonas* sp. M1, and the effects of Ag^+ were more pronounced than those of AgNPs. This different sensitivity of the bacterium to Ag^+ or AgNPs is in agreement with previous findings in aquatic microbes and other species of *Pseudomonas*.[22,53] Short- and long-term exposure (30 min–24 h) to AgNPs led to toxic effects on aquatic Gram-positive and Gram-negative bacteria, although effective concentrations varied widely (45 ng–100 mg).[15] The physicochemical properties of ENPs as well as the exposure time and species sensitivity can contribute to explain such differences.[15] The responses of *Pseudomonas* sp. M1 to each silver form may be different from other strains or species due to putative adaptation to stressors existing in its natural habitat (Rhine River), which has been reported to be occasionally contaminated with metals and organic micropollutants.[54–56] However, adaptive mechanisms of the

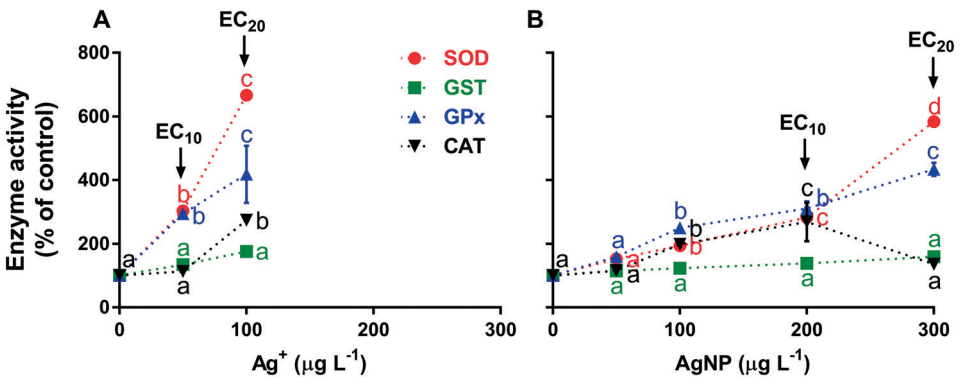

Fig. 2 Activities of SOD, GST, GPx and CAT in *Pseudomonas* sp. M1 exposed at (A) EC_{10} and EC_{20} of Ag^+ and (B) EC_{10} and EC_{20} of AgNPs and at concentrations used for Ag^+. Values are percentages of the respective control. Mean ± SEM, n = 3. Different letters indicate significant differences ($P < 0.05$).

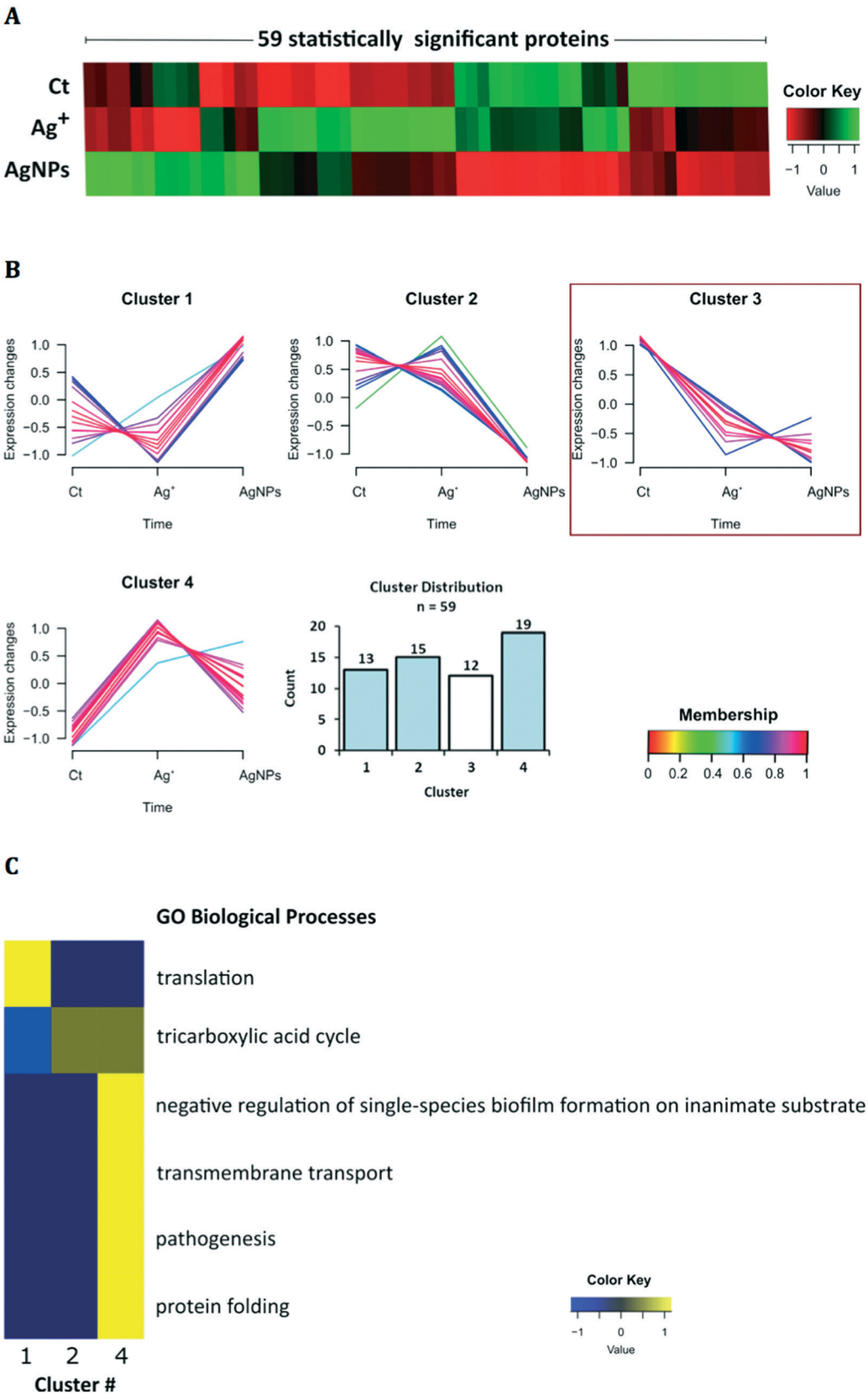

Fig. 3 Heatmap and cluster analysis of changes in proteins in *Pseudomonas* sp. M1 and GO enrichment analysis. The heatmap (A) shows the dynamic profiles of the 59 statistically significant proteins across the different experimental conditions (control, Ct; Ag^+ or AgNPs, NP). The unsupervised cluster analysis (B) was performed considering standardization of the 59 altered proteins. An upper and lower ratio limit of log2 (2) and log2 (0.5) was used for inclusion into a cluster, and the 59 proteins were partitioned into 4 groups where the membership value represents how well the protein profile fits the average cluster profile. (C) Overrepresented biological processes of each cluster. Each cluster from (B) was tested for overrepresented GO compared with cluster 3 using a binomial statistical test with Benjamini–Hochberg adjustment ($P < 0.05$).

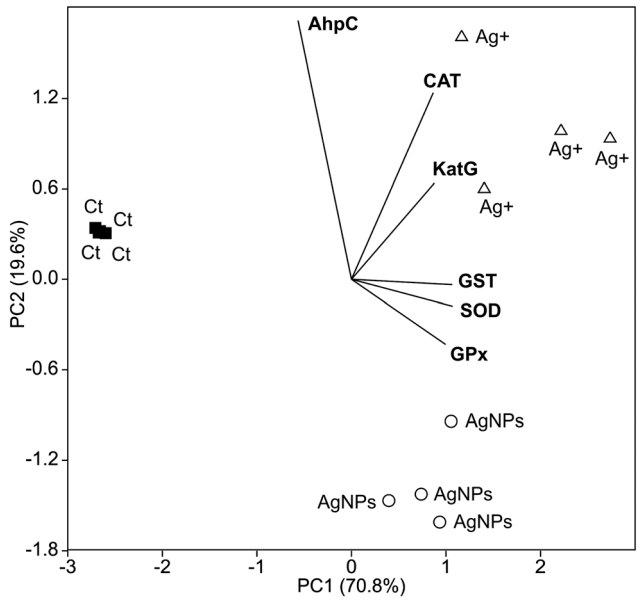

Fig. 4 Principal component analysis (PCA) of proteins involved in antioxidant activities (AhpC and KatG) and activities of antioxidant enzymes (SOD, GST, GPx and CAT) in cells of *Pseudomonas* sp. M1 unexposed or exposed for 90 min to AgNPs or Ag^+ at EC_{20}. Ct: control; AgNPs: 300 μg L^{-1} (~EC_{20}); Ag^+: 100 μg L^{-1} (~EC_{20}).

strain might be specific to the stressors existing in the environment, while the bacterial sensitivity to other stressors might not have been altered. The isolation site of *Pseudomonas* sp. M1 was not contaminated by silver.[54–56] Smaller size AgNPs (1–10 nm) can exhibit toxicity to *P. aeruginosa* by i) impairing membrane permeability and respiration, ii) interacting with sulphur- and phosphorus-containing macromolecules, leading to cellular damage, and iii) releasing Ag^+ leading to additional bactericidal effects.[57] In our study, it is conceivable that the actual toxic effects of AgNPs or Ag^+ on *Pseudomonas* sp. might have been underestimated in the presence of Cl^- in the culture medium. The increased AgNP agglomeration might be the consequence of interactions with the medium components. Therefore, possible interactions between Cl^- and Ag^+ released from AgNPs or $AgNO_3$ cannot be discarded.[17] However, we want to point out that the dissolution of Ag^+ was considerably low at the beginning of our experiment (~0.1%) and decreased further probably due to Ag^+ biosorption to cells. This suggests a low contribution of Ag^+ to the AgNP-induced stress. Moreover, the outcome of the complementary test with cysteine (Fig. S1†), a strong Ag^+ ligand, further supported the theory that AgNPs induced direct toxicity to *Pseudomonas* sp. M1.

Common mechanisms of AgNPs in bactericidal activities involve i) cell wall disruption, ii) interaction with thiol-containing enzymes or peptides, iii) interaction with 30S ribosome and inhibition of protein synthesis, and iv) inhibition of DNA synthesis and induction of apoptosis.[58,59] Our study showed that the short-term exposure of *Pseudomonas* sp. M1 to Ag^+ or AgNPs stimulated the activities of antioxidant enzymes involved in the ascorbate–glutathione cycle, suggesting an attempt of cells to cope with the oxidative stress. The strong response of SOD suggested its crucial role in early defence against ROS, protecting the cells from Ag^+- or AgNP-induced superoxide anion radical ($^{\bullet}O_2^-$), by catalyzing its dismutation into H_2O_2.[12,27] Chronic exposure to AgNPs (0.1–0.25 mg L^{-1}) increased the mRNA of SOD gene in the gill tissue of freshwater fish.[60] However, the exposure to higher concentrations of AgNPs (1–1.5 mg L^{-1}) inhibited SOD activities in *P. aeruginosa* and *P. chlororaphis*, disrupting the antioxidant defence.[35,36] In our study, the induced activities of GPx and CAT by exposure to both Ag forms suggested an efficient cellular detoxification mechanism by scavenging peroxides/hydroperoxides. GPx activity induced by CuONPs was higher in fungi isolated from metal-polluted streams compared to fungi from non-polluted streams, explaining the increase in their tolerance to CuONPs.[27] Higher GPx activity may lead to the scarcity of GSH (reduced glutathione) by its conversion to GSSG (oxidized form), affecting the GSH pool required for cell protection against oxidative stress. Indeed, a considerable decrease in GSH (up to 80%) with exposure to AgNPs (1 mg L^{-1}) induced cytotoxicity in bacteria.[36] In our study, CAT activity increased at the EC_{20} of Ag^+ and the EC_{10} of AgNPs. A decrease in CAT activity was observed in *P. aeruginosa* upon longer exposure (12 h) to higher AgNP concentrations (1 mg L^{-1}),[36] but not under short exposure (1 h) of *P. chlororaphis* to AgNPs (1.5 mg L^{-1}).[35] In our study, GST activity was not triggered by either form of Ag, probably due to the efficient functioning of other antioxidant enzymes in cellular detoxification. The observed positive association between GPx and SOD activities under AgNP exposure suggested the contribution of these enzymes to coping with ROS. The more pronounced activities of antioxidant enzymes under Ag^+ exposure were consistent with the higher toxicity of the ionic form.

Our study provided evidence that Ag^+ and AgNPs affected cellular targets and biological processes in *Pseudomonas* sp. M1. Out of 59 proteins, the contents of which were significantly altered after exposure to either Ag^+ or AgNPs, 15 proteins showed different patterns against each Ag form. The proteomic profiles through GO enrichment analysis based on protein clustering further allowed the exploration of biological processes in *Pseudomonas* sp. M1 and provided the mechanistic insight into the stress induced by Ag^+ or AgNPs (Fig. 3C). The most overrepresented process (12 proteins) under exposure to Ag^+ or AgNPs was the translation, in which 8 proteins increased after exposure to AgNPs but decreased under Ag^+ exposure (cluster 1, Fig. 3C). These proteins were mainly structural constituents of ribosomes which mediate the assembly of small or large ribosomal subunits (*e.g.* 30S ribosomal protein S8, RpsH; see Table S2†) and/or tRNA binding (*e.g.* 30S ribosomal protein S10, RpsJ; see Table S2†). These findings indicated that ionic and nanoparticulate forms of Ag interacted differently with this particular group of proteins. The remaining 4 proteins (clusters 2 and 3) were elongation factors (EFs; *e.g.* Tsf and Tuf, see Table S2†), which decreased under AgNP exposure more than under Ag^+

exposure. The decrease in the content of many elongation factors, including Efp, Tsf and Tuf1 (*e.g.* in *Pseudomonas* sp. M1 under exposure to phenol[40] in *P. stutzeri* exposed to FeNPs[61]), may indicate a compromised protein synthesis due to the stress caused by the nanoparticulate form of Ag. A strong functional association between proteins was obtained in *P. aeruginosa* using STRING database,[62] selecting the networks of the proteins altered by Ag^+ or AgNPs in *Pseudomonas* sp. M1 (Fig. S3†). Moreover, if the polypeptide chain elongation process was affected by AgNPs, defective proteins would be produced and, hence, the performance of the cellular machinery responsible for maintaining protein homeostasis may be altered. In fact, we found an increase in the content of ribosomal constituents under AgNPs exposure which could represent the attempt of cells to counteract incorrect protein formation. Although the process of amino acid synthesis was not featured by GO enrichment analysis, the content of related proteins (*e.g.* LeuC, LeuD and LeuB; cluster 3) decreased under exposure to AgNPs more than to Ag^+, affecting the synthesis of proteins and leucine-based enzyme activities. Indeed, a very strong functional association between LeuD and LeuB was obtained in *P. aeruginosa* using the STRING database when the interaction networks among the proteins altered by Ag^+ or AgNPs in *Pseudomonas* sp. M1 were selected (Fig. S3†). A decrease in the content of proteins involved in amino acid metabolism by Ag^+ and graphene-based AgNPs was reported in *P. aeruginosa*.[63] GO enrichment analysis further supported these findings, demonstrating the importance of other proteins in *Pseudomonas* sp. M1, particularly those associated with the process of protein folding (cluster 4, Fig. 3C) under Ag^+ exposure. This process is accomplished by chaperones, a group of ubiquitous stress responsive proteins that are mainly responsible for proteostasis. Among the functions ensured by these proteins are the prevention of misfolding and promotion of refolding and proper assembly of unfolded polypeptides generated under stress conditions (*e.g.* GroEL, see Table S2†) or the binding to nascent proteins, assisting in their correct folding (*e.g.* DnaK, see Table S2†). STRING analysis of *P. aeruginosa* based on the proteins altered by Ag^+ in *Pseudomonas* sp. M1 showed strong interactions between GroEL and DnaK (Fig. S3†). An increase in GroEL content was also reported in *P. stutzeri* after exposure to FeNPs.[61] DnaK can play a protective role against many stressors, including AgNPs, diminishing the antimicrobial effects and increasing the tolerance of *P. aeruginosa*.[64] Cells of *Pseudomonas* sp. M1 present low levels of these chaperones, but their levels increase under stress, contributing to its tolerance and survival in stressful conditions.[40] Thus, in our study, the increased content of these proteins suggests their involvement in preventing protein misfolding under the stress induced by Ag in *Pseudomonas* sp. M1.

Two of the differentially altered proteins by either forms of Ag had antioxidant roles (KatG and AhpC, see Table S2†) helping to maintain cell-redox homeostasis. Moreover, the activities of CAT and the alterations in the protein content of KatG (1.58-fold for Ag^+ *vs.* 0.74-fold for AgNPs) were closely associated with each other and positively correlated to Ag^+. This suggests that more hydroperoxides were induced by exposure to Ag^+ and that CAT played a crucial role in the cellular detoxification in *Pseudomonas* sp. M1. Increased expression level of catalase (KatA, 1.69-fold) after exposure (24 h) to AgNPs (at 1.2 mg L^{-1}) was also reported in *P. aeruginosa*.[37] AhpC is a key component of a large family of thiol-specific antioxidant proteins known to scavenge reactive oxygen, nitrogen and sulphur species and organic hydroperoxides by reducing to dithiol forms. An increase in the content of AhpC can explain the tolerance of organisms to multiple stressors,[40,65] as observed in *Pseudomonas* sp. after 24 h of exposure to 100 μg L^{-1} AgNPs.[66] In our study, the content of AhpC decreased under the exposure to both forms of Ag, mainly under AgNP exposure (−0.38-fold for Ag^+; −2.68-fold for AgNPs), probably due to shorter exposure to a higher concentration of nanoparticles. Cosgrove *et al.*[67] reported greater catalase expression provoked by a mutation in AhpC, suggesting its compensatory role in oxidative stress. Hence, it is possible that the decrease in the AhpC had occurred in *Pseudomonas* to privilege other antioxidant enzymes against Ag-induced oxidative stress.

In *Pseudomonas* sp. M1, the content of most proteins associated with the tricarboxylic acid cycle (clusters 2 and 4, Fig. 3C) increased under Ag^+ exposure, but decreased under AgNP exposure (*e.g.* aconitate hydratase B – AcnB and isocitrate dehydrogenase [NADP] – Icd), suggesting that different pathways of carbohydrate and energy metabolism were affected by Ag^+ and AgNPs. STRING analysis also showed a strong interaction between AcnB and Icd (Fig. S3†). The exposure to graphene-based AgNPs altered the content of proteins involved in carbohydrate and energy metabolism in *P. aeruginosa*.[63] A decrease in AcnB by other metal NPs was also reported in *P. stutzeri*.[61] In contrast, the increase in the content of those proteins under Ag^+ exposure in *Pseudomonas* sp. M1 suggested an adaptive mechanism in energy consumption and carbohydrate metabolism under Ag stress.

Transmembrane transport was another overrepresented process displayed by GO analysis in *Pseudomonas* sp. M1 (cluster 4) in which proteins (*e.g.* membrane protein, porins and outer membrane protein W, see Table S2†) increased under Ag^+ exposure more strongly than under AgNP exposure. This indicates that these proteins were mainly targeted by Ag^+, affecting the membrane transport and facilitating Ag^+ entrance into bacterial cells.

The processes of pathogenesis and of negative regulation of single-species biofilm formation were also revealed by GO enrichment analysis (cluster 4, Fig. 3C). Although no designation related to this process (as a biological process annotated in UniProt) has been attributed to the proteins belonging to cluster 4, there is evidence that virulence factors related to pathogenesis can also be encoded in the genomes of non-pathogenic bacteria.[68] Moreover, Pitondo-Silva *et al.*[69] demonstrated a co-occurrence of resistance to antibiotics and heavy metals associated with the presence of virulence genes in *P. aeruginosa*, although the influence of other genes and/

or mechanisms related to metal resistance could not be discarded. The process of biofilm formation, whose role in protecting bacteria from antibiotics is well known,[70] was negatively regulated in *Pseudomonas* sp. M1 in our study. Singh *et al.*[71] demonstrated that AgNPs affect the *P. aeruginosa* biofilm by disabling quorum sensing, a communication process used by the strain to regulate virulence and biofilm formation. Because biofilm formation requires a considerable amount of energy in producing extracellular polymeric substances,[72,73] cells of *Pseudomonas* sp. M1 may have prioritized mechanisms/processes (*e.g.* pathogenesis/virulence) to save energy to deal with the stress induced by both silver forms.

Conclusions

Our study showed stronger impacts of the ionic form than the nanoparticulate form of Ag on the growth of *Pseudomonas* sp. M1. However, the low extracellular dissolution of Ag^+ from AgNPs supported the low contribution of dissolved Ag^+ to the stress induced by AgNPs. Our results also demonstrated the involvement of antioxidant enzymes of the ascorbate–glutathione cycle in coping with the oxidative stress induced by both forms of Ag. Proteomic analysis allowed us to identify several proteins, including chaperones, transmembrane transporters, and proteins related to the metabolism of proteins, amino acids, carbohydrates and energy, pointing to them as potential biomarkers of the stress induced by Ag^+ and/or AgNPs. The process of translation was most representative of AgNP exposure, whereas protein folding together with transmembrane transport was the most relevant under Ag^+ exposure. Moreover, it was possible to conclude that each form of Ag induced different adaptive responses in the metabolic, energetic and stress pathways in *Pseudomonas* sp. M1. Overall, our study supports the value of proteomics for elucidating the mechanisms of responses to ENPs and for further assessing the ecotoxicological risk of nanomaterials.

Conflicts of interest

The authors declare no conflict of interests related to this study. They alone are responsible for the contents and writing of the paper. There are no conflicts to declare.

Acknowledgements

This work was supported by the ERDF through the COMPETE2020 – Programa Operacional Competitividade e Internacionalização (POCI) and by the Portuguese Foundation for Science and Technology I.P. (FCT) through the strategic funding UID/BIA/04050/2013 (POCI-01-0145-FEDER-007569), PTDC/AAC-AMB/121650/2010, POCI-01-0145-FEDER-007440 (ref. UID/NEU/04539/2013), the National Mass Spectrometry Network (RNEM) under the contract POCI-01-0145-FEDER-402-022125 (ref. ROTEIRO/0028/2013), and PTDC/BIA-BMA/30922/2017. FCT also supported D. Barros (SFRH/BD/80407/2011). The authors acknowledge S. R. Costa for the final English revision.

References

1 M. E. Vance, T. Kuiken, E. P. Vejerano, S. P. McGinnis, M. F. Hochella Jr., D. Rejeski and M. S. Hull, Nanotechnology in the real world: Redeveloping the nanomaterial consumer products inventory, *Beilstein J. Nanotechnol.*, 2015, **6**, 1769–1780.

2 L. S. Nair and C. T. Laurencin, Biodegradable polymers as biomaterials, *Prog. Polym. Sci.*, 2007, **32**, 762–798.

3 F. Zhang, X. Wu, Y. Chen and H. Lin, Application of silver nanoparticles to cotton fabric as an antibacterial textile finish, *Fibers Polym.*, 2009, **10**, 496–501.

4 S. A. Blaser, M. Scheringer, M. MacLeod and K. Hungerbühler, Estimation of cumulative aquatic exposure and risk due to silver: contribution of nano-functionalized plastics and textiles, *Sci. Total Environ.*, 2008, **390**, 396–409.

5 European Commission, *Commission staff working paper. Types and uses of nanomaterials, including safety aspects. Accompanying the Communication from the Commission to the European Parliament, The Council and the European Economic and Social Committee on the Second Regulatory Review on Nanomaterials*, 2012.

6 R. Kaegi, B. Sinnet, S. Zuleeg, H. Hagendorfer, E. Mueller, R. Vonbank, M. Boller and M. Burkhardt, Release of silver nanoparticles from outdoor facades, *Environ. Pollut.*, 2010, **158**, 2900–2905.

7 K. Tiede, A. B. A. Boxall, X. Wang, D. Gore, D. Tiede, M. Baxter, H. David, S. P. Tear and J. Lewis, Application of hydrodynamic chromatography-ICP-MS to investigate the fate of silver nanoparticles in activated sludge, *J. Anal. At. Spectrom.*, 2010, **25**, 1149–1154.

8 F. Gottschalk, E. Kost and B. Nowack, Engineered nanomaterials in water and soils: a risk quantification based on probabilistic exposure and effect modeling, *Environ. Toxicol. Chem.*, 2013, **32**, 1278–1287.

9 OECD, *Guidance Manual for the testing of manufactured nanomaterials: OECD's sponsorship programme, ENV/JM/MONO (2009) 20REV. OECD Environment, Health and Safety Publications, Series on the Safety of Manufactured Nanomaterials No. 25*, Organisation for Economic Co-operation and Development, Paris, 2010.

10 R. D. Handy, N. van den Brink, M. Chappell, M. Muhling, R. Behra, M. Dusinska, P. Simpson, J. Ahtiainen, A. N. Jha, J. Seiter, A. Bednar, A. Kennedy, T. F. Fernandes and M. Riediker, Practical considerations for conducting ecotoxicity test methods with manufactured nanomaterials: what have we learnt so far?, *Ecotoxicology*, 2012, **21**, 933–972.

11 OECD, *Ecotoxicology and environmental fate of manufactured nanomaterials: test guidelines. Series on the Safety of Manufactured Nanomaterials. No. 40*, ENV/JM/MONO Organisation for Economic Co-operation and Development, Paris, 2014.

12 N. Kumar, G. R. Palmer, V. Shah and V. K. Walker, The effect of silver nanoparticles on seasonal change in arctic tundra bacterial and fungal assemblages, *PLoS One*, 2014, **9**, e99953.

13 E. K. Sohn, S. A. Johari, T. G. Kim, J. K. Kim, E. Kim, J. H. Lee, Y. S. Chung and I. J. Yu, Aquatic Toxicity Comparison of Silver Nanoparticles and Silver Nanowires, *BioMed Res. Int.*, 2015, **2015**, 893049.

14 A. Tlili, J. Cornut, R. Behra, C. Gil-Allué and M. O. Gessner, Harmful effects of silver nanoparticles on a complex detrital model system, *Nanotoxicology*, 2016, **10**, 728–735.

15 J. Fabrega, S. N. Luoma, C. R. Tyler, S. Tamara, T. S. Galloway and J. R. Lead, Silver nanoparticles: behaviour and effects in the aquatic environment, *Environ. Int.*, 2011, **37**, 517–531.

16 Z. Wang, J. W. Chen, X. H. Li, J. P. Shao and W. J. G. M. Peijnenburg, Aquatic toxicity of nanosilver colloids to different trophic organisms: contributions of particles and free silver ion, *Environ. Toxicol. Chem.*, 2012, **31**, 2408–2413.

17 R. Behra, L. Sigg, M. J. Clift, F. Herzog, M. Minghetti, B. Johnston, A. Petri-Fink and B. Rothen-Rutishauser, Bioavailability of silver nanoparticles and ions: from a chemical and biochemical perspective, *J. R. Soc., Interface*, 2013, **10**, 20130396.

18 B. Reidy, A. Haase, A. Luch, K. A. Dawson and I. Lynch, Mechanisms of silver nanoparticle release, transformation and toxicity: a critical review of current knowledge and recommendations for future studies and applications, *Materials*, 2013, **6**, 2295–2350.

19 C. Zhang, Z. Hu and B. Deng, Silver nanoparticles in aquatic environments: Physiochemical behavior and antimicrobial mechanisms, *Water Res.*, 2016, **88**, 403–427.

20 E. McGillicuddy, I. Murray, S. Kavanagh, L. Morrison, A. Fogarty, M. Cormican, P. Dockery, M. Prendergast, N. Rowan and D. Morris, Silver nanoparticles in the environment: Sources, detection and ecotoxicology, *Sci. Total Environ.*, 2017, **575**, 231–246.

21 N. Lubick, Nanosilver toxicity: ions, nanoparticles – or both?, *Environ. Sci. Technol.*, 2008, **42**, 8617.

22 A. Pradhan, S. Seena, C. Pascoal and F. Cássio, Can metal nanoparticles be a threat to microbial decomposers of plant litter in streams?, *Microb. Ecol.*, 2011, **62**, 58–68.

23 S. Cumberland and J. Lead, Particle size distributions of silver nanoparticle at environmentally relevant conditions, *J. Chromatogr. A*, 2009, **1216**, 9099–9105.

24 O. K. Choi and Z. Q. Hu, Nitrification inhibition by silver nanoparticles, *Water Sci. Technol.*, 2009, **59**, 1699–1702.

25 S. Silver, Bacterial silver resistance: molecular biology, *FEMS Microbiol. Rev.*, 2003, **27**, 341–353.

26 M.-M. Azevedo, A. Carvalho, C. Pascoal, F. Rodrigues and F. Cássio, Responses of antioxidant defenses to Cu and Zn stress in two aquatic fungi, *Sci. Total Environ.*, 2007, **377**, 233–243.

27 A. Pradhan, S. Seena, D. Schlosser, K. Gerth, S. Helm, M. Dobritzsch, G.-J. Krauss, D. Dobritzsch, C. Pascoal and F. Cássio, Fungi from metal-polluted streams may have high ability to cope with the oxidative stress induced by copper oxide nanoparticles, *Environ. Toxicol. Chem.*, 2015, **34**, 923–930.

28 A. Pradhan, C. O. Silva, C. Silva, C. Pascoal and F. Cássio, Enzymatic biomarkers can portray nanoCuO-induced oxidative and neuronal stress in freshwater shredders, *Aquat. Toxicol.*, 2016, **180**, 227–235.

29 V. J. Nesatyy and M. J. F. Suter, Proteomics for the analysis of environmental stress responses in organisms, *Environ. Sci. Technol.*, 2007, **41**, 6891–6900.

30 P. Ge, P. Hao, M. Cao, G. Guo, D. Lv, S. Subburaj, X. Li, X. Yan, J. Xiao, W. Ma and Y. Yan, iTRAQ-based quantitative proteomic analysis reveals new metabolic pathways of wheat seedling growth under hydrogen peroxide stress, *Proteomics*, 2013, **13**, 3046–3058.

31 M. C. Teixeira, P. M. Santos, A. R. Fernandes and I. Sá-Correia, Proteome analysis of the yeast response to the herbicide 2,4-dichlorophenoxyacetic acid, *Proteomics*, 2005, **5**, 1889–1901.

32 P. M. Santos and I. Sá-Correia, Characterization of the unique organization and co-regulation of a gene cluster required for phenol and benzene catabolism in *Pseudomonas* sp. M1, *J. Biotechnol.*, 2007, **131**, 371–378.

33 P. M. Santos, T. Simões and I. Sá-Correia, Insights into yeast adaptive response to the agricultural fungicide mancozeb: a toxicoproteomics approach, *Proteomics*, 2009, **9**, 657–670.

34 K. Kalishwaralal, S. BarathManiKanth, S. R. K. Pandian, V. Deepak and S. Gurunathan, Silver nanoparticles impede the biofilm formation by *Pseudomonas aeruginosa* and *Staphylococcus epidermidis*, *Colloids Surf., B*, 2010, **79**, 340–344.

35 C. O. Dimkpa, C. Calder, P. Gajjar, S. Merugu, W. Huang, D. W. Britt, J. E. McLean, W. P. Johnson and A. J. Anderson, Interaction of silver nanoparticles with an environmentally beneficial bacterium, *Pseudomonas chlororaphis*, *J. Hazard. Mater.*, 2011, **188**, 428–435.

36 Y. G. Yuan, Q. L. Peng and S. Gurunathan, Effects of silver nanoparticles on multiple drug-resistant strains of *Staphylococcus aureus* and *Pseudomonas aeruginosa* from mastitis-infected goats: An Alternative Approach for Antimicrobial Therapy, *Int. J. Mol. Sci.*, 2017, **18**, 569.

37 X. Yan, B. He, L. Liu, G. Qu, J. Shi, L. Hu and G. Jiang, Antibacterial mechanism of silver nanoparticles in *Pseudomonas aeruginosa*: proteomics approach, *Metallomics*, 2018, **10**, 557–564.

38 P. M. Santos and I. Sá-Correia, Adaptation to β-myrcene catabolism in *Pseudomonas* sp. M1: An expression proteomics analysis, *Proteomics*, 2009, **9**, 5101–5111.

39 S. Iurescia, A. M. Marconi, D. Tofani, A. Gambacorta, A. Paterno, C. Devirgiliis, M. J. van der Werf and E. Zennaro, Identification and sequencing of beta-myrcene catabolism genes from *Pseudomonas* sp. Strain M1, *Appl. Environ. Microbiol.*, 1999, **65**, 2871–2876.

40 P. M. Santos, V. Roma, D. Benndorf, M. von Bergen, H. Harms and I. Sá-Correia, Mechanistic insights into the global response to phenol in the phenol-biodegrading strain *Pseudomonas* sp. M1, revealed by quantitative proteomics, *OMICS*, 2007, **11**, 233–251.

41 S. Hartmans, J. P. Smits, M. J. van der Werf, F. Volkering and J. A. M. de Bont, Metabolism of styrene oxide and 2-phenylethanol in the styrene-degrading *Xanthobacter* strain 124X, *Appl. Environ. Microbiol.*, 1989, **55**, 2850–2855.

42 G. L. Peterson, Determination of total protein, *Methods Enzymol.*, 1983, **91**, 95–121.

43 A. Clairborne, Catalase activity, in *CRC Handbook of Methods in Oxygen Radical Research*, ed. R. A. Greenwald, CRC Press, Boca Raton FL, 1st edn, 1985, p. 467.

44 L. Flohé and W. A. Günzler, Assays of glutathione peroxidase, *Methods Enzymol.*, 1984, **105**, 114–121.

45 W. H. Habig, M. J. Pabst and W. B. Jakoby, Glutathione S-transferases - first enzymatic step in mercapturic acid formation, *J. Biol. Chem.*, 1974, **249**, 7130–7139.

46 S. I. Anjo, C. Santa and B. Manadas, Short GeLC-SWATH: a fast and reliable quantitative approach for proteomic screenings, *Proteomics*, 2014, **15**, 757–762.

47 B. C. Collins, L. C. Gillet, G. Rosenberger, H. L. Röst, A. Vichalkovski, M. Gstaiger and R. Aebersold, Quantifying protein interaction dynamics by SWATH mass spectrometry: application to the 14-3-3 system, *Nat. Methods*, 2013, **10**(12), 1246–1253.

48 M. Sakuma, Probit analysis of preference data, *Appl. Entomol. Zool.*, 1998, **33**, 339–347.

49 J. H. Zar, *Biostatistical analysis*, Prentice-Hall, Englewood-Cliffs, 2010.

50 K. T. Rigbolt, J. T. Vanselow and B. Blagoev, GProX, a user-friendly platform for bioinformatics analysis and visualization of quantitative proteomics data, *Mol. Cell. Proteomics*, 2011, **10**, O110.007450.

51 L. Kumar and M. E. Futschik, Mfuzz: a software package for soft clustering of microarray data, *Bioinformation*, 2007, **2**, 5–7.

52 Ø. Hammer, D. A. T. Harper and P. D. Ryan, PAST: Paleontological Statistics Software Package for Education and Data Analysis, *Palaeontol. Electron.*, 2001, **4**, 9.

53 O. Bondarenko, A. Ivask, A. Käkinen, I. Kurvet and A. Kahru, Particle-cell contact enhances antibacterial activity of silver nanoparticles, *PLoS One*, 2013, **8**(5), e64060.

54 J. Japenga, K. H. Zschuppe, A. J. DeGroot and W. Salomons, Heavy metals and organic micropollutants in flood plain of the River Waal, a distributary of the River Rhine, 1958-1981, *Neth. J. Agric. Sci.*, 1990, **38**, 381–397.

55 H. Middelkoop, Heavy metal pollution of the river Rhine and Meuse floodplains in the Netherlands, *Neth. J. Geosci.*, 2000, **79**, 411–428.

56 F. A. Vega and L. P. WengP, Speciation of heavy metals in River Rhine, *Water Res.*, 2013, **47**, 363–372.

57 J. R. Morones, J. L. Elechiguerra, A. Camacho, K. Holt, J. B. Kouri, J. T. Ramirez and M. J. Yacaman, The bactericidal effect of silver nanoparticles, *Nanotechnology*, 2005, **16**, 2346–2353.

58 H. Bao, X. Yu, C. Xu, X. Li, Z. Li, D. Wei and Y. Liu, New toxicity mechanism of silver nanoparticles: promoting apoptosis and inhibiting proliferation, *PLoS One*, 2015, **10**, e0122535.

59 P. Dubey, I. Matai, S. U. Kumar, A. Sachdev, B. Bhushan and P. Gopinath, Perturbation of cellular mechanistic system by silver nanoparticle toxicity: Cytotoxic, genotoxic and epigenetic potentials, *Adv. Colloid Interface Sci.*, 2015, **221**, 4–21.

60 S. A. Johari, M. R. Kalbassi, S. B. Lee, M. S. Dong and I. J. Yu, Silver nanoparticles affects the expression of biomarker genes mRNA in rainbow trout (*Oncorhynchus mykiss*), *Comp. Clin. Pathol.*, 2016, **25**, 85–90.

61 M. L. Saccà, C. Fajardo, M. Martinez-Gomariz, G. Costa, M. Nande and M. Martin, Molecular Stress Responses to Nano-Sized Zero-Valent Iron (nZVI) Particles in the Soil Bacterium *Pseudomonas stutzeri*, *PLoS One*, 2014, **9**, e89677.

62 C. von Mering, L. J. Jensen, M. Kuhn, S. Chaffron, T. Doerks, B. Krüger, B. Snel and P. Bork, STRING 7 - recent developments in the integration and prediction of protein interactions, *Nucleic Acids Res.*, 2007, **35**, D358–D362.

63 T. He, H. Liu, Y. Zhou, J. Yang, X. Cheng and H. Shi, Antibacterial effect and proteomic analysis of graphene-based silver nanoparticles on a pathogenic bacterium *Pseudomonas aeruginosa*, *BioMetals*, 2014, **27**, 673–682.

64 K. Markowska, A. M. Grudniak, K. Krawczyk, I. Wróbel and K. I. Wolska, Modulation of antibiotic resistance and induction of a stress response in *Pseudomonas aeruginosa* by silver nanoparticles, *J. Med. Microbiol.*, 2014, **63**, 849–854.

65 Y. Mishra, N. Chaurasia and L. C. Rai, AhpC (alkyl hydroperoxide reductase) from *Anabaena* sp. PCC 7120 protects *Escherichia coli* from multiple abiotic stresses, *Biochem. Biophys. Res. Commun.*, 2009, **381**, 606–611.

66 D. Soni, A. Bafana, D. Gandhi, S. Sivanesan and R. A. Panday, Stress response of *Pseudomonas* species to silver nanoparticles at the molecular level, *Environ. Toxicol. Chem.*, 2014, **33**, 2126–2132.

67 K. Cosgrove, G. Coutts, I. M. Jonsson, A. Tarkowski, J. F. Kokai-kun, J. J. Mond and S. J. Foster, Catalase (KatA) and alkyl hydroperoxide reductase (AhpC) have compensatory roles in peroxide stress resistance and are required for survival, persistence and nasal colonization in *Staphylococcus aureus*, *J. Bacteriol.*, 2007, **189**, 1025–1035.

68 C. Niu, D. Yu, Y. Wang, H. Ren, Y. Jin, W. Zhou, B. Li, Y. Cheng, J. Yue, Z. Gao and L. Liang, Common and pathogen-specific virulence factors are different in function and structure, *Virulence*, 2013, **4**, 473–482.

69 A. Pitondo-Silva, G. B. Gonçalves and E. G. Stehling, Heavy metal resistance and virulence profile in *Pseudomonas aeruginosa* isolated from Brazilian soils, *APMIS*, 2016, **124**, 681–688.

70 N. Høiby, T. Bjarnsholt, M. Givskov, S. Molin and O. Ciofu, Antibiotic resistance of bacterial biofilms, *Int. J. Antimicrob. Agents*, 2010, **35**, 322–332.

71 B. R. Singh, B. N. Singh, A. Singh, W. Khan, A. H. Naqvi and H. B. Singh, Mycofabricated biosilver nanoparticles interrupt *Pseudomonas aeruginosa* quorum sensing systems, *Sci. Rep.*, 2015, **5**, 13719.

72 L. Hall-Stoodley, J. W. Costerton and P. Stoodley, Bacterial biofilms: from the natural environment to infectious diseases, *Nat. Rev. Microbiol.*, 2004, **2**, 95–108.

73 D. López, H. Vlamakis and R. Kolter, Biofilms, *Cold Spring Harbor Perspect. Biol.*, 2010, **2**, a000398.

